

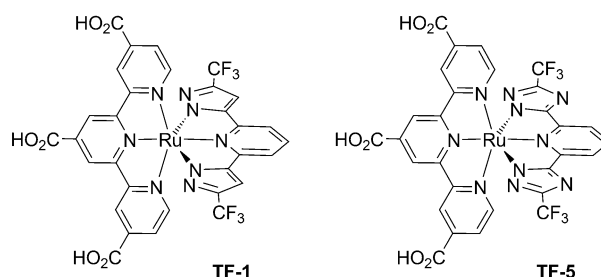
Engineering of Osmium(II)-Based Light Absorbers for Dye-Sensitized Solar Cells**

Kuan-Lin Wu, Shu-Te Ho, Chun-Cheng Chou, Yuh-Chia Chang, Hsiao-An Pan, Yun Chi,* and Pi-Tai Chou*

The light absorber or sensitizer is one of the most important components of dye-sensitized solar cells (DSCs). Adequate engineering of this material allows DSCs to achieve a fine balance among higher solar energy-to-electricity conversion efficiency, lower manufacturing costs, and better long-term stability. The most efficient DSCs to date are fabricated with transition metal based sensitizers.^[1] For example, Grätzel and co-workers recently demonstrated that a Zn^{II} porphyrin with donor-acceptor substituent shows a remarkable power conversion efficiency of $\eta \approx 13\%$ under illumination with standard AM 1.5G simulated sunlight.^[2] Furthermore, many Ru^{II} sensitizers were also known to attain efficiencies greater than 10%,^[3] long before the discovery of the above Zn^{II} dye. Besides these successes, a few quaterpyridine Ru^{II} sensitizers showed notable absorption in the far-red to near-infrared (NIR) region,^[4] with the potential to harvest lower energy photons needed for higher current density.

With a view to harvesting lower energy photons, Os^{II}-based sensitizers seem to be an excellent option for expanding the spectral response well into the NIR region.^[5] First, Os^{II} polypyridine complexes tend to show lower energy metal-to-ligand charge-transfer (MLCT) transition, as a consequence of the lower oxidation potential compared to their Ru^{II} counterparts.^[6] In addition, larger spin-orbit coupling for the heavier Os^{II} cation, in theory, induces nontrivial absorption of the ³MLCT states extended to even lower energy. Thus, appropriately designed Os^{II} sensitizers should display a much broader absorption profile and faster electron injection from both nonthermalized ¹MLCT and thermalized ³MLCT excited states.^[7] We expect that such a photophysical property should be important to both the DSC community and groups whose interests are in developing sensitizers for water splitting with dye-sensitized oxide semiconductors.^[8]

In this study, the design of Os^{II} sensitizers conceptually takes advantage of our previously reported Ru^{II} sensitizer **TF-1**, which contains 4,4',4''-tricarboxy-2,2':6,2''-terpyridine (H₃tctpy) and dianionic 2,6-bis(1,2-pyrazol-5-yl)pyridine chelating ligands (Scheme 1).^[9] This Ru^{II}-based sensitizer showed panchromatic absorption extending to 830 nm and an oxida-



Scheme 1. Ru^{II} sensitizers **TF-1** and **TF-5**.

tion potential of 0.94 V versus the normal hydrogen electrode (NHE) that ensures efficient regeneration of the oxidized sensitizers. However, if the identical architecture were adopted, the oxidation potential of the corresponding Os^{II} sensitizer is predicted to be much less positive.^[6,10] This hurdle can be circumvented by replacing pyrazolate with triazolate with aim of decreasing the electron density at the central Os^{II} ion. This hypothesis is supported by the prior preparation of a relevant triazolate-based Ru^{II} sensitizer, namely, **TF-5** (see Scheme 1). The oxidation potential of **TF-5** is shifted to 1.19 V (vs. NHE), which is 0.25 V higher in energy than that of **TF-1**.

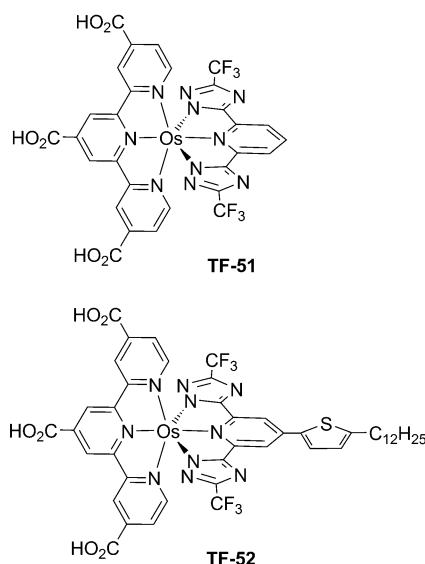
Encouraged by this preliminary result, we focused on the synthesis and characterization of the respective Os^{II} triazolates (see Scheme 2) and DSCs based thereon, which show unprecedented J_{SC} values and the highest overall conversion efficiency among all current Os^{II}-based DSCs.

The required 2,6-bis(3-trifluoromethyl-1H-1,2,4-triazol-5-yl)pyridine ligand was prepared from commercially available pyridine-2,6-dicarbonitrile, followed by triazole cyclization by known procedures.^[11] The 4-thiophene-substituted ligand was synthesized from 4-chloropyridine-2,6-dicarbonitrile by Suzuki coupling, followed by triazole cyclization. The Os^{II} complexes **TF-51** and **TF-52** were obtained by addition of the corresponding 2,6-bis(1,2,4-triazol-5-yl)pyridine to [Os-(tctpy)Cl₃] in xylenes (tctpy = 4,4',4''-tricarboethoxyl-2,2':6',2''-terpyridine). The carboethoxyl groups were then hydrolyzed in basified acetone, followed by acidification to pH 3 to precipitate the products, which were isolated in yields

[*] K.-L. Wu, Dr. S.-T. Ho, C.-C. Chou, Prof. Y. Chi
Department of Chemistry and Low-Carbon Energy Research Center,
National Tsing Hua University
Hsinchu, Taiwan 30013 (R.O.C.)
E-mail: ychi@mx.nthu.edu.tw
Y.-C. Chang, H.-A. Pan, P.-T. Chou
Department of Chemistry and Center for Emerging Material and
Advanced Devices, National Taiwan University
Taipei, Taiwan 10617 (R.O.C.)
E-mail: chop@ntu.edu.tw

[**] This research was supported by National Science Council of Taiwan under grants NSC 100-2119-M-002-008 and NSC-98-3114-E-007-005.

Supporting information for this article is available on the WWW under <http://dx.doi.org/10.1002/anie.201200071>.



Scheme 2. Os^{II} sensitizers **TF-51** and **TF-52**.

of about 40% based on [Os(tcetpy)Cl₃] as limiting reagent, which are comparable to the best yields reported for Os^{II} polypyridine complexes.^[12]

The UV/Vis spectra of Os^{II} sensitizers **TF-51** and **TF-52** in DMF solution are depicted in Figure 1, together with those of Ru^{II} references N749 and **TF-5**. The lowest lying MLCT absorption bands for **TF-51** and **TF-52** are located at 778 and

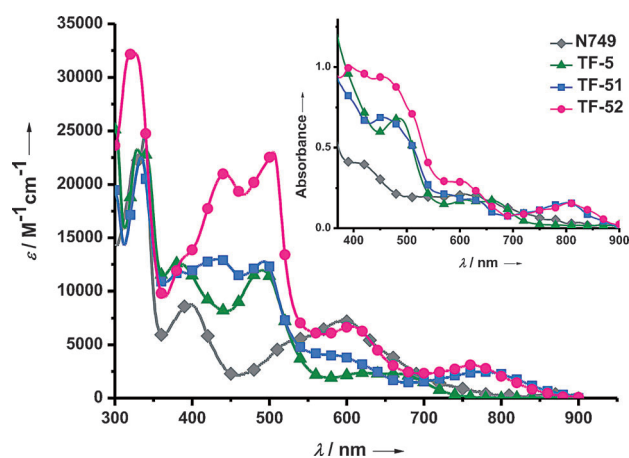


Figure 1. Absorption spectra of **TF-5**, **TF-51**, **TF-52**, and N749 in DMF. Inset: absorption spectra for all samples adsorbed on 6 μm mesoporous TiO₂ thin film.

766 nm with extinction coefficients of 2514 and 3105 L mol⁻¹ cm⁻¹, respectively; both are substantially red-shifted and more intense than those of N749 and **TF-5**. Moreover, dodecylthienyl-substituted sensitizer **TF-52** showed even better absorptivity of those peaks across the whole spectral region. Of equal importance is that the peak at 610 nm showed an equal intensity to the 601 nm signal of N749, which demonstrates the pivotal contribution of thienyl pendant group to enhancing the electronic transitions

and its potential per se as the true panchromatic absorber. The emission spectra of **TF-51** and **TF-52**, which show peak wavelengths of 860 and 856 nm, respectively, are shown in Figure S1 of the Supporting Information. The calculated energy levels for frontier orbitals of **TF-5**, **TF-51**, and **TF-52** that are involved in the S₀→S₁ and S₀→T₁ transitions, the associated orbital transition analyses, and detailed assignment of lower lying electronic transitions based on time-dependent (TD) DFT calculations of all three sensitizers are provided in Table S1 and Figure S2 of the Supporting Information. The lowest lying transition in both singlet and triplet manifolds mainly involves electron transfer from the metal center and 2,6-bis(1,2,4-triazol-5-yl)pyridine ligand to the tricarboxyterpyridine ligand, and hence has substantial MLCT character (> 35%, see Supporting Information Table S1). The calculated S₀→S₁ and S₀→T₁ energy gap for both **TF-51** and **TF-52** extending to about 900 nm are significantly lower than that of **TF-5**, consistent with the UV/Vis absorption measurements.

Cyclic voltammetric data for **TF-51** and **TF-52** are listed in Table 1. The Os²⁺/Os³⁺ oxidation potentials (*E*^{ox}) of **TF-51**

Table 1: Photophysical and electrochemical data of TF sensitizers.

Dye	λ _{abs} [nm] (ε [L mol ⁻¹ cm ⁻¹]) ^[a]	<i>E</i> ^{ox} ^[b]	<i>E</i> ₀₋₀ ^[c]	<i>E</i> ^{ox*} ^[d]
TF-5	340 (22 764), 384 (12 642), 491 (11 955), 667 (2291)	1.19	1.91	-0.72
TF-51	335 (22 503), 382 (11 799), 436 (13 204), 495 (12 767), 601 (3804), 778 (2514)	0.94	1.61	-0.67
TF-52	324 (32 321), 391 (13 305), 444 (20 956), 504 (23 007), 610 (6708), 766 (3105)	0.91	1.61	-0.70
N749	396 (8847), 549 (5813), 601 (7330)	0.89	1.70	-0.81

[a] Absorption and emission spectra were measured in DMF solution.

[b] Oxidation potentials of dyes were measured in DMF with 0.1 M [TBA][PF₆] and at a scan rate of 50 mV s⁻¹. They were calibrated with Fc/Fc⁺ as internal reference and converted to the NHE scale by addition of 0.63 V. [c] *E*₀₋₀ was determined from the intersection of the absorption and tangent of the emission peak in DMF. [d] *E*^{ox*} was calculated as *E*^{ox} - *E*₀₋₀.

and **TF-52** were measured to be 0.94 and 0.91 V, respectively, which are comparable to that of hypothetical I⁻/I₂⁻ couple (ca. 0.79–0.93 V vs. NHE), but are greater than that of I⁻/I₃⁻ (≈ 0.35 V vs. NHE), and hence ensure optimal dye regeneration.^[13] On the other hand, the excited-state oxidation potentials (*E*^{ox*}) of **TF-51** and **TF-52**, derived from both oxidation potential and optical energy gap, are -0.67 and -0.70 V, which are marginally higher than that of the conduction band edge of TiO₂ (-0.5 V vs. NHE). With the lack of sufficient driving voltage for efficient electron injection, it becomes essential to introduce additives such as Li⁺ cation in the electrolyte to further lower the TiO₂ band-edge potential and hence enhancing the photocurrent.

The DSC performance parameters are summarized in Table 2. The corresponding cells were prepared by using a double-layered TiO₂ film, which consisted of a transparent 15 μm absorption layer (composed of 20 nm particles) and a 7 μm scattering layer (composed of 400 nm particles),

Table 2: Performance of DSCs under AM 1.5G one-sun irradiation.

Dye	J_{sc} [mA cm ⁻²]	V_{oc} [V]	FF	η [%]	Notes
TF-5	17.2	0.66	0.715	8.12	[a]
	18.0	0.64	0.716	8.25	[b]
TF-51	17.9	0.57	0.648	6.61	[a]
	20.1	0.56	0.664	7.47	[b]
TF-52	19.7	0.62	0.622	7.60	[a]
	23.3	0.60	0.633	8.85	[b]
N749	20.7	0.60	0.661	8.21	[a]

[a] All devices were fabricated by using a 15 + 7 μ m TiO₂ anode with 4 × 4 mm working area. The dye (0.3 mM) was dissolved in absolute ethanol with 20 vol% DMSO and 0.6 mM of deoxycholic acid. The electrolyte consisted of 0.6 M DMPH, 0.05 M I₂, 0.5 M TBP, and 0.6 M LiI in acetonitrile. Device performance was measured with a 6 × 6 mm shadow mask. [b] The dye solution was alternatively prepared with addition of 2 equiv of [TBA][DOC] to initiate H⁺/TBA⁺ metathesis of sensitizers.

stained with a 0.3 mM dye solution in the presence of 0.6 mM of deoxycholic acid, as this additive is known to improve DSC performance by blocking surface defects.^[14] The electrolyte solution consisted of 0.6 M 1,2-dimethyl-3-propylimidazolium iodide (DMPH), 0.05 M I₂, 0.5 M *tert*-butylpyridine (TBP), and 0.6 M LiI in acetonitrile. The concentration of Li⁺ used in the present study (0.6 M) falls between that reported for typical Ru^{II}-based (0.1 M)^[3b] and Os^{II}-based DSCs (2.0 M).^[5c,d] Thus, a less positive TiO₂ conduction-band potential can be achieved, which, in turn, could afford a higher open-circuit photovoltage V_{oc} , which is also ensured by the addition of 0.5 M of TBP to the electrolyte.^[15] Moreover, higher I⁻ concentration (a total of 1.2 M) in the electrolyte is expected to offset the higher electron concentration in TiO₂ and to impede the undesired recombination between electrons in TiO₂ and oxidized sensitizers.^[16]

Under full sunlight irradiation (AM 1.5G, 100 mW cm⁻²), the **TF-52**-sensitized device exhibited a short-circuit photocurrent density J_{sc} of 19.7 mA cm⁻², a V_{oc} of 0.62 V, and a fill factor (FF) of 0.622, corresponding to a power conversion efficiency η of 7.60%. Since the neutral **TF-52** dye has an excited-state oxidation potential close to the conduction band of TiO₂, electron injection would not be optimal. To compensate this unfavorable situation, we then added 2 equiv of tetrabutylammonium deoxycholate [TBA][DOC] to the dye solution, so that in situ metathesis of carboxylic acid/carboxylate anion of dyes can take place in the dye solution to raise the virtual oxidation potential of the excited sensitizers.^[17] As expected, this maneuver increased J_{sc} to 23.3 mA cm⁻² and FF to 0.633, but slightly decreased V_{oc} to 0.60 V at the same time, giving an enhanced efficiency of η = 8.85%. To provide further support for this approach, DSCs employing regular Ru^{II} sensitizer **TF-5** and Os^{II} sensitizer **TF-51** gave conversion efficiencies of 8.25 and 7.47%, respectively. After H⁺/TBA⁺ metathesis, Os^{II} sensitizer **TF-51** also showed a much larger enhancement of 0.86% versus that of the less affected Ru^{II} sensitizer **TF-5** (0.13%). Despite the small variation of E^{o*} values between **TF-5** and **TF-51**, the invariance of the latter is interesting. Due to the heavier Os^{II} atom and hence faster rate of intersystem crossing, it is likely that excited **TF-51** ejects an electron mainly from the lowest lying ³MLCT state. Conversely, the Ru^{II} counterpart **TF-5**, on

excitation, may eject an electron from either ¹MLCT or ³MLCT state. Thermodynamically, the ¹MLCT state lies substantially higher in energy than the TiO₂ conduction band, and thus the difference is much less affected by in situ deprotonation of carboxyl anchors.

The J - V characteristics and IPCE action spectra of devices employing the TBA⁺-exchanged sensitizers are shown in Figure 2a and b. In the IPCE spectrum, **TF-52** obviously covers a wider spectral response from 380 to 960 nm and reaches a maximum of 78% at 480 nm, whereas

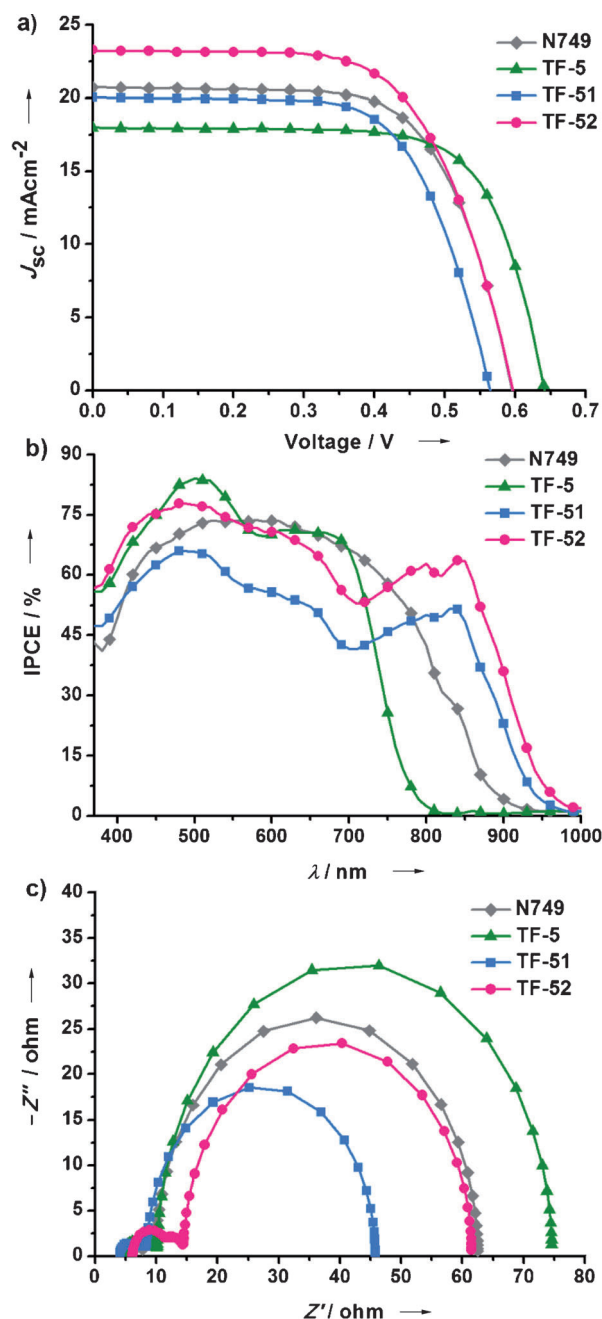


Figure 2. a) J - V characteristics measured under AM 1.5 conditions, b) Incident photon-to-electron conversion efficiency (IPCE) action spectra, and c) electrochemical impedance spectra measured in the dark at a forward bias of 0.6 V for the cells employing various TF dyes and N749.

the Ru^{II} reference **TF-5** displays a maximum of 83 % at 510 nm and tails off at only 800 nm.

Electrochemical impedance spectroscopy (EIS) was performed in the dark and with a forward bias of 0.6 V. The Nyquist plots of DSCs based on different sensitizers are shown in Figure 2c. Two semicircles from left to right in the Nyquist plot represent the impedances of charge transfer (R_{Pt}) on the Pt counterelectrode and charge recombination (R_{r}) at the interface of the TiO₂/electrolyte.^[18] As a result, the radius of the second semicircle reveals a descending order of **TF-5** > **N749** ≈ **TF-52** > **TF-51**, which is consistent with the trend of V_{OC} values (see Table 2). A smaller R_{r} value indicates faster electron recombination from TiO₂ to electron acceptors in an electrolyte and thus results in lower V_{OC} . The results also manifest the advantage of molecular engineering from **TF-51** to **TF-52**.

For testing long-term stability, a high performance electrolyte based on butyronitrile (BN) was selected.^[19] Over the entire 1000 h testing period at 60 °C under one-sun light soaking, the photovoltaic parameters J_{SC} , V_{OC} , FF of the **TF-52** based cell varied only slightly from the initial values (Figure 3). The final η retained 97 % of its initial value, that is, a small drop of V_{OC} by 40 mV is compensated by an increase in J_{SC} . Such an impressive performance is remarkable and is among the best that ever documented in the literature.

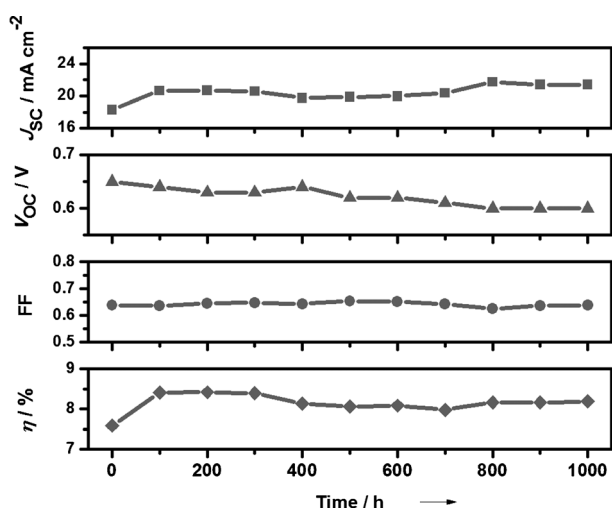


Figure 3. Evolution of solar-cell parameters of **TF-52** under AM 1.5G light soaking at 60 °C.

In summary, we have demonstrated that Os^{II}-based sensitizers can be used to construct highly efficient DSCs, particularly when a moderate excess of LiI was incorporated into the electrolyte to promote electron injection into TiO₂. Our experiments give a comprehensive guideline, not only to achieving panchromatic absorption, but also to controlling the energy difference of the TiO₂ band edge and E°_{ox} of the sensitizer and the gap between the redox potential of I[−]/I₃[−] couple and E°_{ox} of the sensitizer. The successful design of Os^{II}-based sensitizers in combination with their capability to display both panchromatic absorption and high optical

density should pave an alternative route to the summit of DSC efficiency.

Received: January 4, 2012

Revised: February 27, 2012

Published online: April 24, 2012

Keywords: chelates · N ligands · osmium · solar cells · tridentate ligands

- a) L. M. Gonçalves, V. de Zea Bermudez, H. A. Ribeiro, A. M. Mendes, *Energy Environ. Sci.* **2008**, *1*, 655; b) M. Grätzel, *Acc. Chem. Res.* **2009**, *42*, 1788; c) Y. Luo, D. Li, Q. Meng, *Adv. Mater.* **2009**, *21*, 4647; d) A. Hagfeldt, G. Boschloo, L. Sun, L. Kloo, H. Pettersson, *Chem. Rev.* **2010**, *110*, 6595.
- A. Yella, H.-W. Lee, H. N. Tsao, C. Yi, A. K. Chandiran, M. K. Nazeeruddin, E. W.-G. Diau, C.-Y. Yeh, S. M. Zakeeruddin, M. Grätzel, *Science* **2011**, *334*, 629.
- a) M. K. Nazeeruddin, P. Pechy, T. Renouard, S. M. Zakeeruddin, R. Humphry-Baker, P. Comte, P. Liska, L. Cevey, E. Costa, V. Shklover, L. Spiccia, G. B. Deacon, C. A. Bignozzi, M. Grätzel, *J. Am. Chem. Soc.* **2001**, *123*, 1613; b) Q. Yu, S. Liu, M. Zhang, N. Cai, Y. Wang, P. Wang, *J. Phys. Chem. C* **2009**, *113*, 14559; c) J.-J. Kim, H. Choi, C. Kim, M.-S. Kang, H.-S. Kang, J. Ko, *Chem. Mater.* **2009**, *21*, 5719; d) M. Wang, S.-J. Moon, D. Zhou, F. Le Formal, N.-L. Cevey-Ha, R. Humphry-Baker, C. Grätzel, P. Wang, S. M. Zakeeruddin, M. Grätzel, *Adv. Funct. Mater.* **2010**, *20*, 1821; e) A. Reynal, E. Palomares, *Eur. J. Inorg. Chem.* **2011**, 4509; f) K.-L. Wu, H.-C. Hsu, K. Chen, Y. Chi, M.-W. Chung, W.-H. Liu, P.-T. Chou, *Chem. Commun.* **2010**, 5124; g) S.-H. Yang, K.-L. Wu, Y. Chi, Y.-M. Cheng, P.-T. Chou, *Angew. Chem.* **2011**, *123*, 8420; *Angew. Chem. Int. Ed.* **2011**, *50*, 8270.
- a) A. Abboto, F. Sauvage, C. Barolo, F. De Angelis, S. Fantacci, M. Grätzel, N. Manfredi, C. Marinzi, M. K. Nazeeruddin, *Dalton Trans.* **2011**, *40*, 234; b) Q.-J. Pan, Y.-R. Guo, L. Li, S. O. Odoh, H.-G. Fu, H.-X. Zhang, *Phys. Chem. Chem. Phys.* **2011**, *13*, 14481.
- a) G. Sauvé, M. E. Cass, G. Coia, S. J. Doig, I. Lauermaun, K. E. Pomykal, N. S. Lewis, *J. Phys. Chem. B* **2000**, *104*, 6821; b) S. Altobello, R. Argazzi, S. Caramori, C. Contado, S. Da Fre, P. Rubino, C. Chone, G. Larramona, C. A. Bignozzi, *J. Am. Chem. Soc.* **2005**, *127*, 15342; c) A. C. Onicha, F. N. Castellano, *J. Phys. Chem. C* **2010**, *114*, 6831; d) T. Yamaguchi, T. Miyabe, T. Ono, H. Arakawa, *Chem. Commun.* **2010**, 5802.
- a) P.-T. Chou, Y. Chi, *Eur. J. Inorg. Chem.* **2006**, 3319; b) Y. Chi, P.-T. Chou, *Chem. Soc. Rev.* **2007**, *36*, 1421.
- S. Verma, P. Kar, A. Das, D. K. Palit, H. N. Ghosh, *Chem. Eur. J.* **2010**, *16*, 611.
- W. J. Youngblood, S.-H. A. Lee, K. Maeda, T. E. Mallouk, *Acc. Chem. Res.* **2009**, *42*, 1966.
- C.-C. Chou, K.-L. Wu, Y. Chi, W.-P. Hu, S. J. Yu, G.-H. Lee, C.-L. Lin, P.-T. Chou, *Angew. Chem.* **2011**, *123*, 2102; *Angew. Chem. Int. Ed.* **2011**, *50*, 2054.
- M. Alebbi, C. A. Bignozzi, T. A. Heimer, G. M. Hasselmann, G. J. Meyer, *J. Phys. Chem. B* **1998**, *102*, 7577.
- H.-Y. Hsieh, C.-H. Lin, G.-M. Tu, Y. Chi, G.-H. Lee, *Inorg. Chim. Acta* **2009**, *362*, 4734.
- E. Z. Jandrasics, F. R. Keene, *J. Chem. Soc. Dalton Trans.* **1997**, 153.
- a) D. Kuciauskas, M. S. Freund, H. B. Gray, J. R. Winkler, N. S. Lewis, *J. Phys. Chem. B* **2001**, *105*, 392; b) J. N. Clifford, E. Palomares, M. K. Nazeeruddin, M. Grätzel, J. R. Durrant, *J. Phys. Chem. C* **2007**, *111*, 6561; c) A. Listorti, B. O'Regan, J. R.

- Durrant, *Chem. Mater.* **2011**, 23, 3381; d) G. Boschloo, E. A. Gibson, A. Hagfeldt, *J. Phys. Chem. Lett.* **2011**, 2, 3016.
- [14] T. Daeneke, T.-H. Kwon, A. B. Holmes, N. W. Duffy, U. Bach, L. Spiccia, *Nat. Chem.* **2011**, 3, 211.
- [15] S. Zhang, X. Yang, K. Zhang, H. Chen, M. Yanagida, L. Han, *Phys. Chem. Chem. Phys.* **2011**, 13, 19310.
- [16] A. Y. Anderson, P. R. F. Barnes, J. R. Durrant, B. C. O'Regan, *J. Phys. Chem. C* **2011**, 115, 2439.
- [17] a) M. K. Nazeeruddin, R. Humphry-Baker, P. Liska, M. Grätzel, *J. Phys. Chem. B* **2003**, 107, 8981; b) N. R. Neale, N. Kopidakis, J. van de Lagemaat, M. Grätzel, A. J. Frank, *J. Phys. Chem. B* **2005**, 109, 23183.
- [18] F. Fabregat-Santiago, J. Bisquert, G. Garcia-Belmonte, G. Boschloo, A. Hagfeldt, *Sol. Energy Mater. Sol. Cells* **2005**, 87, 117.
- [19] F. Sauvage, S. Chhor, A. Marchioro, J.-E. Moser, M. Grätzel, *J. Am. Chem. Soc.* **2011**, 133, 13103.
-